NANOSYSTEMS

S.V. KONDOVYCH,[1] H.V. GOMONAY,[1] V.M. LOKTEV[2]

[1] National Technical University of Ukraine "Kyiv Polytechnic Institute"
 (37, Peremogy Ave., Kyiv 03056, Ukraine; e-mail: ksvitlana@i.ua)
[2] Bogolyubov Institute for Theoretical Physics, Nat. Acad. of Sci. of Ukraine
 (14b, Metrolohichna Str., Kyiv 03680, Ukraine)

PACS 75.85.+t, 75.70.-i,
75.50.Ee, 77.65.-j, 76.50.+g

MAGNETIC DYNAMICS OF A MULTIFERROIC WITH AN ANTIFERROMAGNETIC LAYER

Shape effects in magnetic particles are widely studied, because of the ability of the shape and the size to control the parameters of a sample during its production. Experiments with nano-sized samples show that the shape can affect also the properties of antiferromagnetic (AFM) materials. However, the theoretical interpretation of these effects is under discussion. A model to study the shape-induced effects in AFM particles at the AFM resonance frequency is proposed. The Lagrange function method is used to calculate the spectrum of resonance oscillations of the AFM vector in a synthetic multiferroic (piezoelectric + antiferromagnet). The influence of the specimen shape on the AFM resonance frequency in the presence of an external magnetic field is studied. Conditions for a resonance under the action of an external force or for a parametric resonance to arise in the magnetic subsystem are considered.

K e y w o r d s: antiferromagnet, piezoelectric, multiferroic, nanoparticles, Lagrangian.

1. Introduction

Although the influence of the shape of ferromagnetic nanoparticles on their magnetic properties has been widely studied [1–3], the shape effects for nano-dimensional AFM particles remain a matter of discussion. In works [4–6], the effect of AFM vector reorientation from a direction corresponding to the crystallographic "easy" axis to a direction induced by a prolate particle was experimentally observed. This fact enables us to talk about shape effects in antiferromagnets.

The majority of available methods used to observe the domain structure in AFM materials and determine the AFM vector orientation – such as the X-ray polarization spectroscopy, the second harmonic generation, and so forth – are intended to research static effects. Often, they do not take the influence of the dimensions and the shape of a specimen on its magnetic properties into account. We suggest that

a resonance method should be used for studying the dynamics of the AFM vector. We will show that the shape-induced magnetic anisotropy in AFM crystals can be analyzed with the help of the AFM resonance spectrum or a spectrum of one of the long-wave quasi-particle excitations. A significant contribution to the theory of the latter was made by the outstanding Soviet and Ukrainian scientist O.S. Davydov [7]. This work is dedicated to the centennial anniversary of his birthday.

More specifically, the work is aimed at studying a synthetic multiferroic that combines AFM and piezo-electric (PE) properties. The purposes of the work are (i) to study the influence of time-dependent (periodic) deformations of a piezoelectric subsystem on the magnetic subsystem in the AFM/PE multiferroic, (ii) to determine conditions, under which forced resonance oscillations or a parametric resonance can arise in the specimen, and (iii) to analyze the dependence of resonance frequencies on the geometrical parameters of the system in the presence of an external magnetic field.

The main idea of the work consists in that we affect the elastic subsystem of an AFM nanoparticle in order to study the dynamics of its magnetic subsystem – namely, long-wave oscillations of the AFM vector – and to analyze the contribution of the shape-induced magnetic anisotropy. In so doing, we suppose that the mechanism of influence of the shape on the magnetic anisotropy of AFM nanoparticles has a magnetoelastic character, being governed by the so-called "destressing energy" [8].

Note that the influence of the specimen shape on the AFM vector dynamics was studied earlier. In particular, in work [9], the dependence of the gap, which is a result of the shape-induced anisotropy, in the AFM resonance spectrum on the direction of an applied external magnetic field has been analyzed. In this work, a more complicated situation is considered, because the proposed approach makes allowance for both the magnetic and elastic subsystems in the AFM specimen. The perturbations in the magnetoelastic system are simulated as those induced by an ac electric voltage applied across a synthetic AFM/PE multiferroic. Besides the specimen shape, the external electric and magnetic fields play the role of control parameters.

2. Model and Method

2.1. Researched specimen

Consider a two-layer synthetic material fabricated by sputtering an AFM film onto a PE substrate (Fig. 1, *a*). To simplify the model, we consider that the antiferromagnet is collinear, including two equivalent sublattices characterized by the magnetic moments $\mathbf{M}_1$ and $\mathbf{M}_2$. Let the specimen have an elliptic shape with the semiaxis lengths a and b, and let the AFM film thickness be equal to h, with $a > b \gg h$. The dimensions of the AFM subsystem are supposed to be small enough, so that it can be considered in the "macrospin" approximation, i.e. the dynamics of a uniform single-domain layer can be analyzed. At temperatures below the Néel one, the magnetic state of this system can be completely described with the use of the AFM vector $\mathbf{L} = \mathbf{M}_1 - \mathbf{M}_2$ with a fixed length $|\mathbf{L}| = 2M_0$.

Under the action of an external electric voltage V, there emerges a mechanical stress in the piezoelectric, described by the stress tensor $\sigma \sim Vd$, where d is the piezoelectric tensor. This stress brings about a
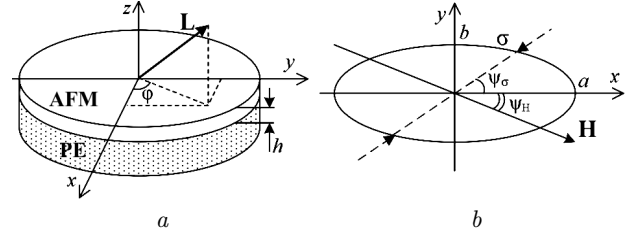

Fig. 1. AFM film with thickness h sputtered onto the PE substrate (*a*). The AFM vector $\mathbf{L}$ (the thick arrow) characterizes the magnetic state of the system. Specimen has the elliptic shape with the semiaxis lengths a and b (*b*). Dashed arrows denote the direction (the angle ψ_σ) of the force that creates a mechanical stress in the specimen. The direction of strength lines of the external magnetic field $\mathbf{H}$ is shown by the thin arrow, the corresponding angle is ψ_H

specimen deformation $u_0 = \sigma_0/(2\mu)$, where μ is the shear modulus, and σ_0 the component of the stress tensor in the direction of the external force (at the angle ψ_σ with respect to the Ox axis, see Fig. 1, *b*). The external magnetic field $\mathbf{H} = H\left(\cos\psi_\text{H}, \sin\psi_\text{H}, 0\right)$ lies in the xOy plane (Fig. 1, *b*).

2.2. Lagrangian

In order to calculate the AFM resonance spectrum, let us use a standard technique based on the Lagrange function method (e.g., see [10]). The Lagrangian density for the AFM specimen equals

$$\mathcal{L}_\text{AFM} = \frac{\chi}{2g^2 M_0^2}\dot{\mathbf{L}}^2 - \frac{\chi}{2gM_0^2}(\dot{\mathbf{L}}, \mathbf{L}, \mathbf{H}) +$$

$$+ \frac{\chi}{8M_0^2}[\mathbf{L} \times \mathbf{H}]^2 - w_\text{an}(\mathbf{L}) - w_\text{destr} - \Delta w_\text{destr}(\sigma), \quad (1)$$

where g is the gyromagnetic ratio; χ the magnetic susceptibility of the material;

$$w_\text{an}(\mathbf{L}) = \frac{K_\parallel}{4M_0^2}L_z^2 - \frac{K_\perp}{16M_0^4}(L_x^4 + L_y^4) \quad (2)$$

is the density of the magnetic anisotropy energy for an AFM of the "easy plane" type [1]; $K_\parallel \gg K_\perp > 0$ are the anisotropy constants;

$$w_\text{destr} = \frac{1}{2}\left\{\frac{K_\parallel^\text{el}}{4M_0^2}(L_y^2 - L_x^2) + \frac{K_\text{is}^\text{el}}{16M_0^4}\left[\left(L_x^2 - L_y^2\right)^2 + \right.\right.$$

$$\left.\left. + 4\left(L_x L_y\right)^2\right] - \frac{K_\perp^\text{el}}{16M_0^4}\left[\left(L_x^2 - L_y^2\right)^2 - 4\left(L_x L_y\right)^2\right]\right\} \quad (3)$$

---

[1] Anisotropy energy (2) corresponds to the tetragonal symmetry of a magnetic ordering in the AFM layer.

is the destressing energy density [2] [8]; $K_{\parallel}^{\mathrm{el}}$, $K_{\mathrm{is}}^{\mathrm{el}}$, and $K_{\perp}^{\mathrm{el}}$ are the magnetoelastic coefficients depending on the specimen shape (see Appendix); and

$$\Delta w_{\mathrm{destr}}(\sigma) = \frac{1}{4\mu}\sigma_0 \cos 2\psi_{\sigma}\left\{(K_{\parallel}^{\mathrm{el}} + \Delta K_{\parallel})\frac{L_y^2 - L_x^2}{4M_0^2} - \right.$$
$$\left. - (K_{\perp}^{\mathrm{el}} + \Delta K_{\perp})\frac{(L_x^2 - L_y^2)^2 - 4(L_x L_y)^2}{16M_0^4}\right\} \quad (4)$$

is a correction to w_{destr} that arises under the influence of an external stress owing to a variation of the specimen shape at a deformation [11] (expressions for $\Delta K_{\parallel,\perp}$ can be found in Appendix).

2.3. Parametrization of the AFM vector

Let us examine the emergence of resonance oscillations of the AFM vector **L** in a vicinity of its equilibrium position $\mathbf{L}_{\mathrm{eq}}$ and analyze the influence of the specimen shape on its resonance frequencies. In the absence of external fields, the AFM vector lies in the xOy plane, and it can be parametrized by the angle φ_{eq} with respect to the Ox axis: $\mathbf{L}_{\mathrm{eq}} = 2M_0\,(\cos\varphi_{\mathrm{eq}}, \sin\varphi_{\mathrm{eq}}, 0)$. If the crystallographic axes in the material are directed along the ellipse axes, and the magnetoelastic contribution (Eqs. (3) and (4)) is not taken into account, this angle can be equal to $\varphi_{\mathrm{eq1}} = 0$ or $\varphi_{\mathrm{eq2}} = \pi/2$; in the general case, the angle φ_{eq} can accept an arbitrary value. The external magnetic field also affects the orientation of AFM vector.

Let the structures of the crystal lattices in the AFM and PE substances coincide, and let the substrate deformation invoked by an external electric voltage be transferred into the AFM film, which results in a small rotation of the AFM vector, $\mathbf{L} = \mathbf{L}_{\mathrm{eq}} + \mathbf{l}$, where $|\mathbf{l}| \ll |\mathbf{L}_{\mathrm{eq}}|$ and $\mathbf{l} \perp \mathbf{L}_{\mathrm{eq}}$. Then it is convenient to introduce the following parametrization for the vector **L**:

$$L_x = 2M_0 \cos\varphi_{\mathrm{eq}}(1 - l_\perp^2/2 - l_\parallel^2/2) - 2M_0 l_\perp \sin\varphi_{\mathrm{eq}};$$
$$L_y = 2M_0 \sin\varphi_{\mathrm{eq}}(1 - l_\perp^2/2 - l_\parallel^2/2) + 2M_0 l_\perp \cos\varphi_{\mathrm{eq}};$$
$$L_z = 2M_0 l_\parallel. \quad (5)$$

Here, $l_\perp$ and $l_\parallel$ are the projections of the vector **l** on the plane and the Oz axis, respectively.

---

[2] Destressing energy (3) is written down for a single-domain film (i.e. the geometrical dimensions of the specimen are supposed to be small enough, so that a non-uniformity of the magnetic subsystem can be neglected) and assuming that the elastic properties of the crystal are isotropic.

3. Oscillations of the AFM Vector under the Action of an External Force

Let the AFM/PE specimen be unstrained in the absence of external fields. We express the alternating mechanical stress that arises in the specimen under the action of an external electric voltage with frequency ω in the form $\sigma(t) = \mathrm{Re}\left\{\sigma_0 e^{i\omega t}\right\}$ and suppose the amplitude σ_0 to be small. Being determined from the standard procedure of potential energy minimization, the stable equilibrium states of the AFM vector (they are parametrized by the angles φ_{eq}) satisfy the relations

$$(2K_\perp + 4K_\perp^{\mathrm{el}*})\sin 4\varphi_{\mathrm{eq}} + 2K_\parallel^{\mathrm{el}*}\sin 2\varphi_{\mathrm{eq}} -$$
$$- \chi H^2 \sin 2(\varphi_{\mathrm{eq}} - \psi_{\mathrm{H}}) = 0; \quad (6)$$

$$\Omega_\perp^2 \equiv \frac{g^2}{2\chi}\left[(2K_\perp + 4K_\perp^{\mathrm{el}*})\cos 4\varphi_{\mathrm{eq}} + K_\parallel^{\mathrm{el}*}\cos 2\varphi_{\mathrm{eq}} - \right.$$
$$\left. - \frac{1}{2}\chi\mathrm{H}^2 \cos 2(\varphi_{\mathrm{eq}} - \psi_{\mathrm{H}})\right] \geq 0; \quad \Omega_\parallel^2 \approx \frac{g^2 K_\parallel}{2\chi} \geq 0, \quad (7)$$

where the quantities $\Omega_\perp$ and $\Omega_\parallel$ coincide with the frequencies of characteristic free oscillations of the AFM vector in the specimen plane and perpendicularly to it, respectively (see below). The magnetoelastic coefficients $K_\parallel^{\mathrm{el}*}$ and $K_\perp^{\mathrm{el}*}$ include corrections $\Delta K_{\parallel,\perp}$ that arise under the action of a mechanical stress $\sigma(t)$ applied in the ψ_σ-direction,

$$K_\parallel^{\mathrm{el}*} = K_\parallel^{\mathrm{el}} + \frac{1}{2\mu}\sigma(K_\parallel^{\mathrm{el}} + \Delta K_\parallel)\cos 2\psi_\sigma;$$
$$\quad (8)$$
$$K_\perp^{\mathrm{el}*} = K_\perp^{\mathrm{el}} + \frac{1}{2\mu}\sigma\left(K_\perp^{\mathrm{el}} + \Delta K_\perp\right)\cos 2\psi_\sigma.$$

In order to obtain the equations describing the AFM vector oscillations, let us parametrize Lagrangian (1) and pass to small deviations $l_\perp$ and $l_\parallel$ from the equilibrium positions (see Eq. (5)). Taking expression (6) for equilibrium states of the AFM vector into account and neglecting the terms proportional to $\sigma_0 l_\perp^2$ and $\sigma_0 l_\parallel^2$ as the quantities of the third order of smallness, we obtain the Lagrange equations

$$\ddot{l}_\perp + 2\gamma_{\mathrm{AFM}}\dot{l}_\perp - \Omega_{\mathrm{H}}\dot{l}_\parallel + \Omega_\perp^2 l_\perp = -\Phi\sigma_0 e^{i\omega t};$$
$$\quad (9)$$
$$\ddot{l}_\parallel + 2\gamma_{\mathrm{AFM}}\dot{l}_\parallel + \Omega_{\mathrm{H}}\dot{l}_\perp + \Omega_\parallel^2 l_\parallel = 0.$$

The coefficient γ_{AFM} is the AFM resonance width; it simulates the damping of oscillations. In Eqs. (9), the following notations wwere introduced:

$$\Omega_{\mathrm{H}} = g\mathrm{H}\cos(\varphi_{\mathrm{eq}} - \psi_{\mathrm{H}});$$

$$\Phi \equiv \Phi\left(\Delta K_{\|,\perp}, \varphi_{\mathrm{eq}}, \psi_\sigma\right) = \frac{1}{8\mu}\frac{g^2}{\chi}\Bigg[\left(K_\|^{\mathrm{el}*} + \Delta K_\|\right) \times$$

$$\times \sin 2\varphi_{\mathrm{eq}} + 2\left(K_\perp^{\mathrm{el}*} + \Delta K_\perp\right)\sin 4\varphi_{\mathrm{eq}}\Bigg]\cos 2\psi_\sigma,$$

φ_{eq} is the solution of Eq. (6), and the angles ψ_{H} and ψ_σ are defined above (see Fig. 1, *b*). The function Φ in Eq. (9) makes allowance for a variation of the specimen shape at a deformation and modifies the magnitude of external influence. By changing the angle ψ_σ that determines the specimen deformation direction, it is possible to control the amplitude of AFM vector oscillations. The frequencies $\Omega_\perp$ and $\Omega_\|$ are the frequencies of characteristic oscillations of the AFM vector components $l_\perp$ and $l_\|$, respectively. They are different for different equilibrium orientations of the vector **L** and depend on both the magnetoelastic constants and the magnetic field **H**. Note that $\Omega_\| \gg \Omega_\perp$, because $K_\| \gg K_\perp$.

The resonance in the AFM/PE system arises at the frequencies

$$\omega^2 = \omega_{1,2}^2 = \frac{1}{2}\Bigg(\Omega_\perp^2 + \Omega_\|^2 + \Omega_{\mathrm{H}}^2 - 2\gamma_{\mathrm{AFM}}^2 \pm$$

$$\pm \sqrt{\left(\Omega_\perp^2 + \Omega_\|^2 + \Omega_{\mathrm{H}}^2\right)^2 - 4\Omega_\perp^2\Omega_\|^2 - 4\gamma_{\mathrm{AFM}}^2\Omega_{\mathrm{H}}^2}\Bigg). \quad (10)$$

In the absence of a magnetic field, there exist four different equilibrium orientations of the AFM vector in a single-domain specimen (they can be obtained from Eq. (6) with **H** = 0),

$$\varphi_{\mathrm{eq1}} = 0; \quad \varphi_{\mathrm{eq2}} = \frac{\pi}{2};$$
$$\cos 2\varphi_{\mathrm{eq3,4}} = \frac{-K_\|^{\mathrm{el}*}}{\left(2K_\perp + 4K_\perp^{\mathrm{el}*}\right)}. \quad (11)$$

The stability of the equilibrium states (11) was studied in work [11]. Note that no more than two orientations of the vector **L** can be stable simultaneously (see Fig. 2): either at the angles $\varphi_{\mathrm{eq1,2}}$ or the angles $\varphi_{\mathrm{eq3,4}}$. If the ellipse is prolate and the ratio between the lengths of its semiaxes exceeds a certain critical value $(a/b)_{\mathrm{crit}}$ [8], there exists only one stable equilibrium orientation for the AFM vector–along the Ox axis.

For definiteness, let the specimen be deformed along the longer ellipse axis ($\psi_\sigma = 0$). The deformation-induced modification of the specimen shape affects the behavior of the magnetic system, and this
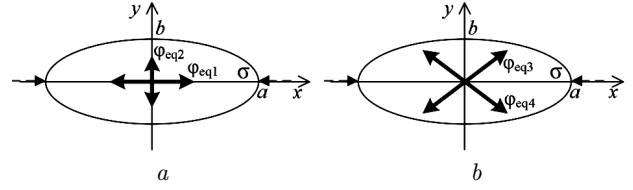

Fig. 2. Equilibrium orientations of the AFM vector. Dashed arrows denote the specimen deformation direction (along the Ox axis). Thick arrows correspond to the states of the AFM vector that can be stable simultaneously: (*a*) at the angles $\varphi_{\mathrm{eq1}} = 0$ and $\varphi_{\mathrm{eq2}} = \pi/2$ and (*b*) at the angles $\varphi_{\mathrm{eq3,4}}$ (see Eq. (11)) with respect to the Ox axis

influence depends on the stable state, in which the AFM vector dwells. In a vicinity of the equilibrium orientation at the angle $\varphi_{\mathrm{eq1}} = 0$ or $\varphi_{\mathrm{eq2}} = \pi/2$, there is no resonance under the action of an external force, because $\Phi = 0$ in the system of equations (9). A deformation will result in only a shift of characteristic oscillation frequencies $\Omega_\perp$ and $\Omega_\|$ according to corrections in Eq. (8).

At the same time, the emergence of oscillations in the AFM/PE system owing to the shape change is possible in a vicinity of the equilibrium angles $\varphi_{\mathrm{eq3,4}}$ (Fig. 2,*b*). The effective projection of a mechanical stress σ deflects the AFM vector from its stable equilibrium orientation, and resonance oscillations of the vector **L** in the specimen plane can occur even in the absence of a magnetic field (Fig. 3).

It should be emphasized that, for the resonance to take place under such conditions, the geometry of the system and the relative directions between the axes of an elliptic specimen and the crystallographic axes of material must be selected carefully to provide the condition $K_\perp^{\mathrm{el}} < 0$, which is responsible for the stability of "diagonal" equilibrium positions. The analysis of Eq. (9) with a non-zero magnetic field shows that the oscillations of individual AFM vector components become "entangled", so that the vector **L** oscillates both in the specimen plane and perpendicularly to it. Neglecting the oscillation damping ($\gamma_{\mathrm{AFM}} = 0$) and writing down the corresponding solutions for the components of the AFM vector in the forms

$$l_\perp = \frac{\Phi\sigma_0\left(\omega^2 - \Omega_\|^2\right)}{\left(\omega^2 - \Omega_\perp^2\right)\left(\omega^2 - \Omega_\|^2\right) - \Omega_{\mathrm{H}}^2\omega^2}\cos\omega t;$$

$$l_\| = -\frac{\Phi\sigma_0\Omega_{\mathrm{H}}\omega}{\left(\omega^2 - \Omega_\perp^2\right)\left(\omega^2 - \Omega_\|^2\right) - \Omega_{\mathrm{H}}^2\omega^2}\sin\omega t, \quad (12)$$
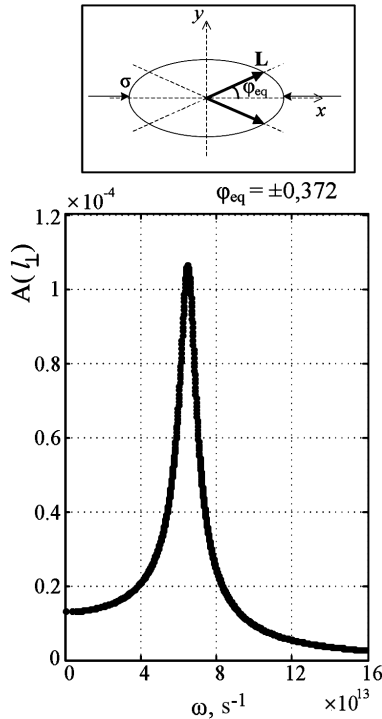
Fig. 3. Amplitude-frequency characteristic of oscillations of the AFM vector **L**. The external magnetic field is absent. $A(l_\perp)$ is the amplitude of a relative deviation of the vector **L** from the equilibrium orientation. The inset: the vector **L** (the thick arrow) oscillates in the xOy plane, the angles φ_{eq} correspond to the stable equilibrium orientations of the vector **L**, thin arrows denote the direction of an external mechanical stress σ (along the Ox axis, $\psi_\sigma = 0$). Simulation was carried out for an NiO AFM particle with the ratio between the ellipse semiaxis lengths $a/b = 20$. The other model parameters are quoted in Table

Physical characteristics of NiO antiferromagnet used in the simulation (see works [8, 12–14] and Appendix)

Parameter	$a/b = 2.4$	$a/b = 20$
χ	1.28×10^{-3}	
g, s^{-1}/T	$2.5\gamma_e = 4.4 \times 10^{11}$	
$K_\parallel$, J/m^3	500	
$K_\perp$, J/m^3	28.8	
$K_\parallel^{el}$, J/m^3	20	90
$|K_\perp^{el}|$, J/m^3	5	45

one can immediately see that the application of an external magnetic field changes the character of oscillations. Namely, instead of two linearly polar-

ized modes (a "soft" mode in the xOy plane and a "rigid" one perpendicularly to it), the oscillations of the vector **L** are described by elliptically polarized modes, whose ellipticity degree depends on **H**. Figure 4 demonstrates the difference of the oscillation amplitudes for the components $l_\perp$ and $l_\parallel$. The resonance frequencies of those modes depend on the equilibrium AFM vector orientation, in a vicinity of which the vector oscillates, and are given by expression (10).

If $\mathbf{H} \neq 0$, the equilibrium orientations of the AFM vector change; namely, the magnetic field rotates the vector **L** (see insets in Fig. 4). Let the equilibrium position of the AFM vector in a vicinity of 0 be designated as φ_{eq1} and near $\pi/2$ as φ_{eq2}; those angles are the solutions of Eq. (6). Figure 4 exhibits the amplitude-frequency characteristics of oscillations in a vicinity of the equilibrium states φ_{eq1} and φ_{eq2}. The values of maximum positions (resonance frequencies (10)) are changed if the specimen shape is involved in the Lagrangian (it is so because the corrections $\Delta K_{\parallel, \perp}$ depend on the ratio a/b between the ellipse semiaxis lengths, which parametrizes the specimen shape). The orientation of the AFM vector is determined not only by the directions of the crystallographic axes and the direction of an external magnetic field, but also by the direction of the "easy" axis given by the particle shape (along the larger ellipse axis). The shape-induced uniaxial magnetic anisotropy eliminates the energy degeneration among various equilibrium states of the AFM vector (in the infinite-specimen approximation and in the absence of external fields, the states $\varphi = 0$ and $\varphi = \pi/2$ are equivalent), and the frequencies of oscillations near those equilibrium orientations become split.

The dependences of the oscillation frequencies on the direction and the magnitude of an external magnetic field, as well as on the elliptic specimen shape, are depicted in Fig. 5. The figure demonstrates a number of regularities:

1. The specimen shape, being parametrized by the ratio between the ellipse semiaxis lengths a/b, affects the magnitudes of resonance frequencies. When comparing cases a and c in Fig. 5, one can see that the "soft" mode frequency ω_2 becomes almost twice as large if the eccentricity a/b increases. The "rigid" mode frequency ω_1 remains almost constant at that. This fact follows from that the deformation makes a
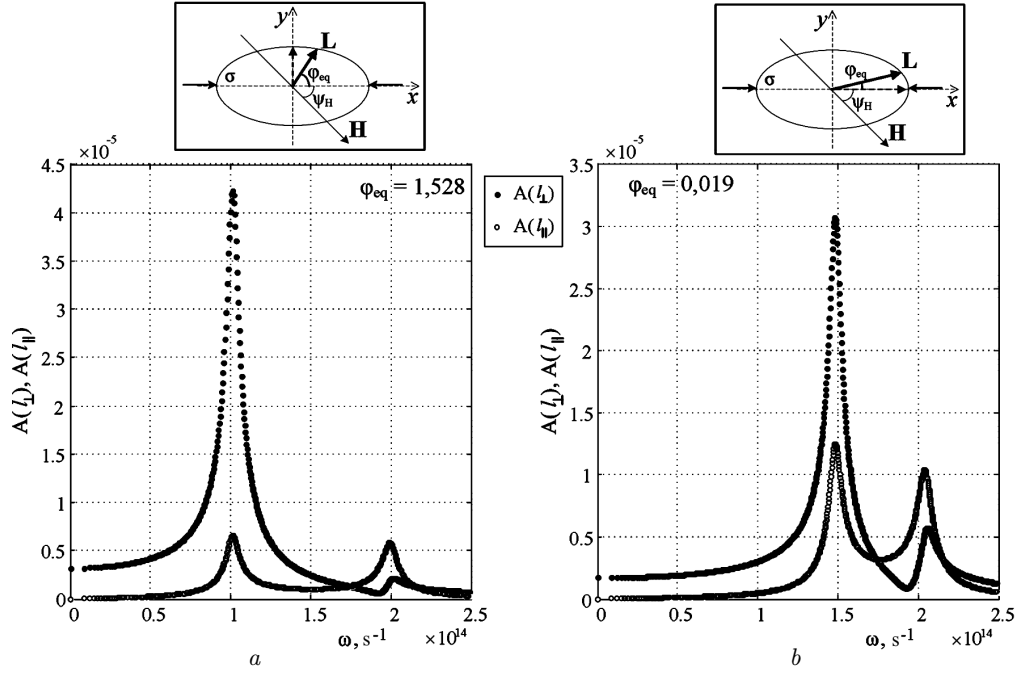
Fig. 4. Amplitude-frequency characteristics of oscillations of the AFM vector **L** in a magnetic field calculated from expression (10). $A(l_\perp)$ and $A(l_\parallel)$ are the amplitudes of relative deviations of the vector **L** from equilibrium orientations in the xOy plane and along the Oz axis, respectively. Panels (a) and (b) correspond to different equilibrium orientations of the AFM vector (6) schematically indicated *in the insets* by dashed arrows. Thin arrows *in the insets* denote the direction of an external mechanical stress σ (along the Ox axis, $\psi_\sigma = 0$). Simulation was carried out for an NiO AFM particle with the ratio between the ellipse semiaxis lengths $a/b = 20$. The other model parameters are quoted in Table. The external magnetic field **H** is directed at the angle $\psi_H = -\pi/4$. $H = 100$ Oe $\approx 7.7 \times 10^3$ A/m

larger correction to $K_\parallel^{\mathrm{el}}$ than to $K_\perp^{\mathrm{el}}$ (8) as the parameter a/b increases.

2. The "soft" modes are more sensitive to anisotropy. It is clear because the dependences on the magnetic field direction are stretched along different directions for different equilibrium states. The axis, along which the angular diagram is stretched, corresponds to the state with lower energy (the mutually perpendicular orientations of the vectors **H** and **L**).

3. If the parameter a/b grows, the frequency ω_2 of AFM vector oscillations in a vicinity of $\varphi_{\mathrm{eq2}} = \pi/2$ decreases at certain magnetic field directions (the angle ψ_H). This is evidenced by a bending of the angular diagrams in Figs. 5, b and d. The obtained dependence allows the influence of the AFM/PE specimen shape on the dynamics of its magnetic subsystem to be examined.

4. Parametric Resonance

Let us demonstrate that there may emerge a parametric resonance in the AFM/PE system in the pres-

ence of an ac electric field. For this purpose, we retain terms down to the $\sigma_0 l_\perp^2$ and $\sigma_0 l_\parallel^2$ orders of smallness in the Lagrange equations (9) and present the mechanical stress that arises in the system owing to the application of ac electric voltage in the form $\sigma(t) = \sigma_0 \cos \omega t$. As a result, we obtain the equations

$$\ddot{l}_\perp + 2\gamma_{\mathrm{AFM}} \dot{l}_\perp - \Omega_H \dot{l}_\parallel + \Omega_\perp^2 \left(1 + \frac{\sigma_0 \Phi_\perp}{\Omega_\perp^2} \cos \omega t\right) l_\perp = 0;$$

$$\ddot{l}_\parallel + 2\gamma_{\mathrm{AFM}} \dot{l}_\parallel + \Omega_H \dot{l}_\perp + \Omega_\parallel^2 \left(1 + \frac{\sigma_0 \Phi_\parallel}{\Omega_\parallel^2} \cos \omega t\right) l_\parallel = 0,$$

$$(13)$$

where $\Phi_\perp$ and $\Phi_\parallel$ are some functions of the magnetoelastic coefficients $K_{\perp,\parallel}^{\mathrm{el}}$, corrections $\Delta K_{\parallel,\perp}$, direction ψ_σ of the external voltage application, and equilibrium state of the AFM vector, in a vicinity of which the resonance oscillations (the solutions of Eq. (6)) are observed.
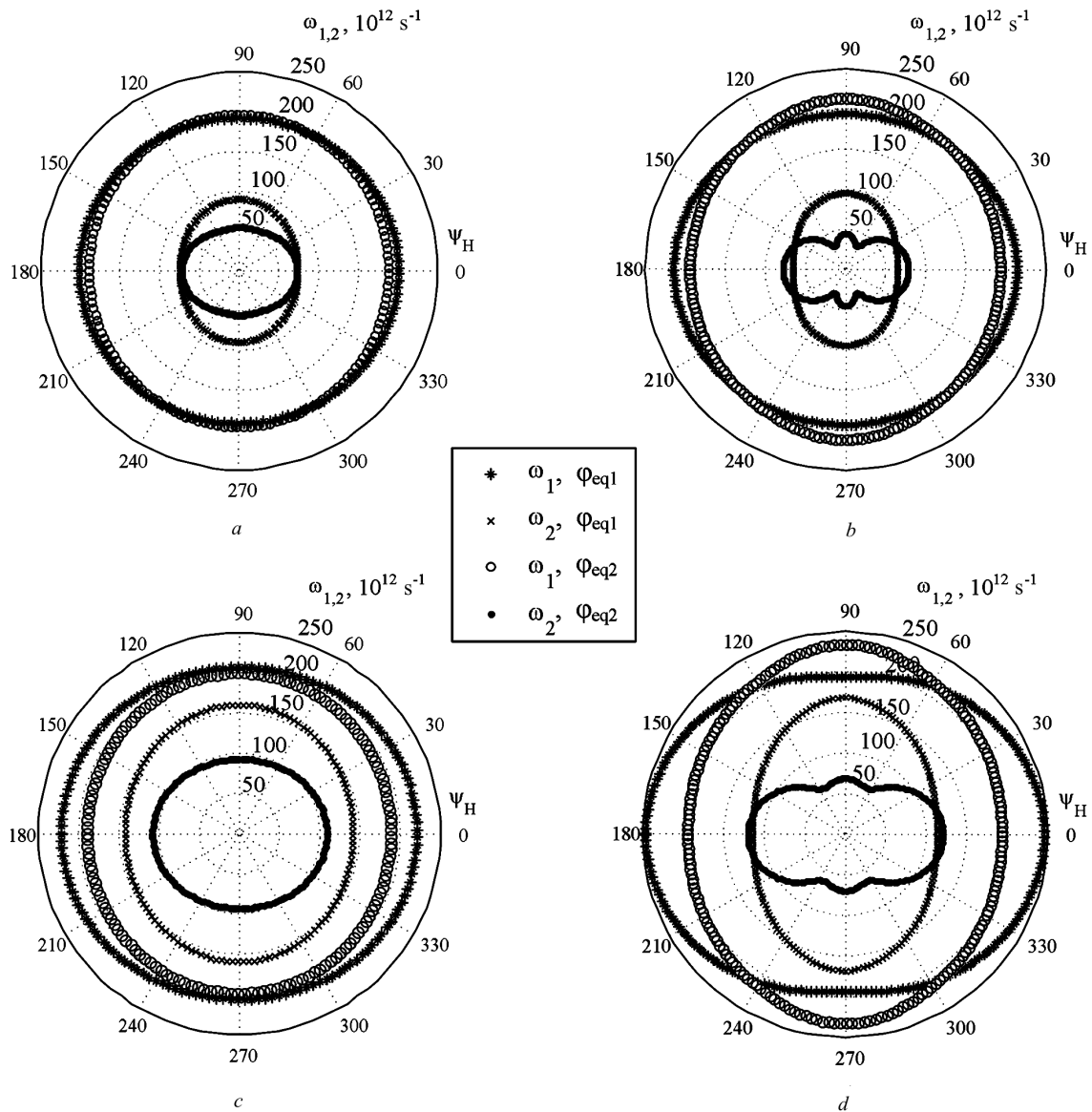
Fig. 5. Dependences of oscillation frequencies $\omega_{1,2}$ of the AFM vector in a vicinity of two different equilibrium states φ_{eq1} and φ_{eq2} (see the insets in Fig. 4) on the magnetic field direction (the angle ψ_{H}) calculated by formula (10). Panels (*a*) and (*b*) correspond to a specimen with the ratio between its semiaxis lengths $a/b = 2.4$, and panels (*c*) and (*d*) to $a/b = 20$. The magnetic field strength $H = 100$ (*a* and *c*), 140 (*b*), and 200 Oe (4). Simulation was carried out for an NiO AFM particle. The model parameters are quoted in Table

In the absence of a magnetic field ($\Omega_{\mathrm{H}} = 0$), the oscillation equations (13) are independent. Each of the equations acquires a standard form of the Mathieu equation [15]. The parametric resonance with the largest band width arises at the frequencies

$$\omega = 2\Omega_{\perp} \pm \Delta\omega_{\perp}/2; \quad \omega = 2\Omega_{\parallel} \pm \Delta\omega_{\parallel}/2.$$

Here, the first band width for the AFM vector component $l_{\perp}$ equals

$$\Delta\omega_{\perp} = 2\sqrt{(\sigma_0 \Phi_{\perp}/2\Omega_{\perp})^2 - 4\gamma_{\mathrm{AFM}}^2}$$

and, for component $l_{\parallel}$,

$$\Delta\omega_{\parallel} = 2\sqrt{(\sigma_0 \Phi_{\parallel}/2\Omega_{\parallel})^2 - 4\gamma_{\mathrm{AFM}}^2}.$$

Since $\Omega_{\parallel} \gg \Omega_{\perp}$, it becomes clear that it is rather a difficult task to excite parametric resonances in the plane and perpendicularly to it simultaneously. The width $\Delta\Omega_{\parallel}$ of the first resonance band for oscillations along the Oz axis is narrower in comparison with that for in-plane oscillations. This is a consequence of the facts that the studied antiferromagnetic is of the "easy plane" type, and the oscillation mode along the Oz axis is more rigid.

The dependence of the resonance band width on $\Phi_{\perp,\parallel}$ allows one to regulate the resonance width by selecting the specimen shape.

The parametric resonance also arises in a vicinity of the frequencies $\omega = 2\Omega_{\perp}/n$ and $\omega = 2\Omega_{\parallel}/n$, where $n = 1, 2, 3, \ldots$. The band widths decrease at that, by following the rules $(\Delta\omega_{\perp})_n^2 \sim (\sigma_0/\Omega_{\perp}^2)^{2n}$ and $(\Delta\omega_{\parallel})_n^2 \sim (\sigma_0/\Omega_{\parallel}^2)^{2n}$.

The considered partial case can be realized not only when $\mathbf{H} = 0$, but also when $\mathbf{H}$ is oriented perpendicularly to either of the AFM specimen easy axes (along the Ox or Oy axis). Then, the vector $\mathbf{L}$ will be in the equilibrium position at either $\varphi_{\mathrm{eq1}} = 0$ or $\varphi_{\mathrm{eq}} = \pi/2$, respectively.

In the presence of a magnetic field ($\mathbf{H} \neq 0$), the complete system of equations (13) is to be solved. For this purpose, let us first change to normal oscillation modes $Q_{1,2}$. The characteristic frequencies of normal oscillations coincide with the parameters $\omega_{1,2}$ in expression (10). We apply the Floquet theorem and seek the solutions in the form

$$Q_1 \sim \exp(i\beta t) \sum_n a_n \exp(i\omega n t);$$

$$Q_2 \sim \exp(i\beta t) \sum_n b_n \exp(i\omega n t).$$

As a result, we obtain a system of equations for the coefficients a_n and b_n. Using this system to study the parametric resonance, e.g., in a vicinity of $\omega \approx \omega_1$ (for $n = 2$), we obtain the following formula for the resonance band width:

$$\Delta\omega_{(n=2)} \approx 2\sqrt{\left(\frac{\sigma_0^2 \Phi_{\perp}^2}{8\omega_1^3}\right)^2 - 4\gamma_{\mathrm{AFM}}^2}.$$

Hence, the band width of the parametric resonance for oscillations of the vector $\mathbf{L}$ in an AFM particle can be controlled by both changing the geometrical parameters of the particle (this way allows the magnitudes of resonance frequencies to be adjusted already

at the specimen fabrication stage) and applying external fields, electric and/or magnetic ones.

5. Discussion and Conclusions

In this work, the influence of the shape of AFM particles on their resonance properties has been studied. The proposed model of AFM/PE multiferroic allows both elastic and magnetic properties of the system to be considered simultaneously. The combination of a piezoelectric and an antiferromagnet in the same specimen makes it possible to control the system state by means of electric and magnetic fields.

It is shown that there emerges an additional uniaxial magnetic anisotropy in the AFM/PE system, which depends on the specimen shape. This anisotropy makes one of the antiferromagnet's "easy" axes (they are formed by either the orientation of crystallographic axes or the application of an external magnetic field) more beneficial energetically, i.e. it eliminates the degeneration between two equivalent equilibrium orientations of the AFM vector.

AFM vector oscillations near the stable equilibrium vector orientation can be excited in a number of cases. In the absence of external fields, if the antiferromagnet's "easy" axis does not coincide with the easy axes induced by the specimen shape (for instance, along the ellipse axes), the specimen deformation can favor the rotation of the AFM vector to a more energetically beneficial direction. If an ac electric voltage is additionally applied to the AFM/PE particle, it gives rise to the emergence of ac mechanical stresses in and, consequently, the varying deformation of the particle. As a result, the AFM vector executes small oscillations in the specimen plane (Fig. 3).

For a certain geometry of the system, the mechanical stress cannot induce resonance oscillations of the AFM vector, namely, when the stress is applied along one of the "easy" axes (see Fig. 2, *a*). The external magnetic field rotates the vector $\mathbf{L}$ and causes the appearance of an effective projection of the mechanical stress and, as a result, the oscillations of the AFM vector owing to the varying deformation of the specimen (Fig. 4). Moreover, the magnetic field entangles the "soft" mode of in-plane oscillations with the "rigid" mode that is perpendicular to it, so that the oscillations of the vector $\mathbf{L}$ become elliptically polarized.

It is of importance that the frequencies of AFM vector resonance oscillations depend on the specimen

shape (for example, on the ratio a/b between the ellipse semiaxis lengths) and on the magnitude and the direction of an external magnetic field (Fig. 5). This circumstance allows the properties of an AFM particle to be controlled and predicted already at the particle fabrication stage; in particular, it is possible to select particle's shape and dimensions, as well as the corresponding orientation of the crystallographic axes in the specimen plane, depending on the particle usage specificity.

We have also demonstrated a possibility to excite a parametric resonance in the AFM/PE system. The band width of the parametric resonance is governed by both the magnitude of mechanical stress induced in the specimen and the specimen shape. Hence, by choosing the shape and the dimensions of a specimen, it is possible to control the region, where the parametric resonance emerge at variable deformations.

To summarize, we note that the dependences obtained in this work can be used for a direct experimental verification of the shape effect in antiferromagnets.

APPENDIX
Magnetoelastic Coefficients
and the Corresponding Corrections That Take
the Specimen Shape into Account

For an elliptic nanofilm ($a > b \gg h$), the magnetoelastic coefficients look like [8]

$$K_\parallel^{\text{el}} = \frac{h}{b} \frac{[(\lambda')^2(2 - 3\nu) + \lambda_v \lambda'] J_\parallel(k)}{4\mu(1 - \nu)},$$

$$K_{\text{is}}^{\text{el}} = \frac{(\lambda')^2(3 - 4\nu)}{8\mu(1 - \nu)}, \qquad K_\perp^{\text{el}} = \frac{h}{b} \frac{2(\lambda')^2 J_\perp(k)}{3\mu(1 - \nu)},$$

where μ is the shear modulus, ν is Poisson's ratio, and λ_v and λ' are magnetoelastic moduli. The shape integrals $J_\parallel(k)$ and $J_\perp(k)$ depend on the specimen geometry by means of the parameter $k^2 = 1 - b^2/a^2$ as follows:

$$J_\parallel(k) = \int_0^{\pi/2} \frac{(k^2 \sin^2\phi + \cos 2\phi)d\phi}{\sqrt{1 - k^2 \sin^2\phi}},$$

$$J_\perp(k) = \int_0^{\pi/2} \frac{(1 - 8\cos 2\phi - k^2 \sin^2\phi + 8\cos 2\phi/k^2)d\phi}{\sqrt{1 - k^2 \sin^2\phi}}.$$

Elastic deformation of a specimen modifies the anisotropy constants of the second and fourth orders and contributes to the destressing energy (4). The corrections $\Delta K_{\parallel,\perp}$ depend on the linear sizes of the specimen and the shape integrals in the following manner [11]:

$$\Delta K_\parallel = 4\frac{h}{b} \frac{[(\lambda')^2(2 - 3\nu) + \lambda_v \lambda']}{4\mu(1 - \nu)}(1 - k^2)\frac{dJ_\parallel(k)}{d(k^2)},$$

$$\Delta K_\perp = 4\frac{h}{b} \frac{2(\lambda')^2}{3\mu(1 - \nu)}(1 - k^2)\frac{dJ_\perp(k)}{d(k^2)}.$$

The introduction of those corrections allows one to study how a change of the specimen shape affects the state of the magnetic subsystem in an AFM/PE multiferroic.

1. R.P. Cowburn, J. Phys. D: Appl. Phys. **33**, R1 (2000).
2. E.Y. Vedmedenko, H.P. Oepen, and J. Kirschner, J. Magn. Magn. Mater. **256**, 237 (2003).
3. Yi Li, Yiran Lu, and W.E. Bailey, J. Appl. Phys. **113**, 17B506 (2013).
4. E. Folven, T. Tybell, A. Scholl, A. Young, S.T. Retterer, Y. Takamura, and J.K. Grepstad, Nano Lett. **10**, 4578 (2010).
5. E. Folven, A. Scholl, A. Young, S.T. Retterer, J.E. Boschker, T. Tybell, Y. Takamura, and J.K. Grepstad, Phys. Rev. B **84**, 220410 (2011).
6. E. Folven, A. Scholl, A. Young, S.T. Retterer, J.E. Boschker, T. Tybell, Y. Takamura, and J.K. Grepstad, Nano Lett. **12**, 2386 (2012).
7. A.S. Davydov, *Theory of Molecular Excitons* (Plenum Press, New York, 1971).
8. H.V. Gomonay and V.M. Loktev, Phys. Rev. B **75**, 174439 (2007).
9. H.V. Gomonay, E.G. Kornienko, and V.M. Loktev, Ukr. J. Phys. **50**, 816 (2005).
10. E.A. Turov, A.V. Kolchanov, V.V. Menshenin, I.F. Mirsaev, and V.V. Nikolaev, *Symmetry and Physical Properties of Antiferromagnets* (Fizmatlit, Moscow, 2001) (in Russian).
11. S.V. Kondovych and H.V. Gomonay, Visn. Lviv. Univ. Ser. Fiz. **47**, 159 (2012).
12. P. de V. Du Plessis, S.J. van Tonder, and L. Alberts, J. Phys. C **4**, 1983 (1971).
13. P. de V. Du Plessis, S.J. van Tonder, and L. Alberts, J. Phys. C **4**, 2565 (1971).
14. M.T. Hutchings and E.J. Samuelsen, Phys. Rev. B **6**, 3447 (1972).
15. L.D. Landau and E.M. Lifshitz, *Mechanics* (Butterworth-Heinemann, Oxford, 2001).

С.В. Кондович, О.В. Гомонай, В.М. Локтев

МАГНІТНА ДИНАМІКА МУЛЬТИФЕРОЇКА
З АНТИФЕРОМАГНІТНИМ ПРОШАРКОМ

Р е з ю м е

Ефекти форми для магнітних частинок інтенсивно дослі-
джуються, адже форма і розміри можуть виступати в ро-
лі керуючих параметрів і задавати властивості зразка вже
при його виготовленні. Експерименти дозволяють припу-
стити існування впливу форми на властивості антиферо-
магнітних (АФМ) нанорозмірних зразків, але з теоретичної
точки зору цей вплив майже не розглянуто. В даній робо-
ті запропоновано модель для дослідження впливу ефектів
форми в АФМ частинках на частоті антиферомагнітного
резонансу (АФМР). Методом функцій Лагранжа розрахо-
вано спектр резонансних коливань АФМ вектора для син-
тетичного мультифероїка (п'єзоелектрик + АФМ). Дослі-
джено вплив форми зразка на частоту АФМР у присутності
зовнішнього магнітного поля. Розглянуто умови, за яких в
магнітній підсистемі виникає: а) резонанс під дією зовні-
шньої примусової сили; б) параметричний резонанс.